Transient Flow into a Partially Penetrating Well during the Constant-Head Test in Unconfined Aquifers

Ya-Chi Chang[1]; Geng-Yuan Chen[2]; and Hund-Der Yeh, Aff.M.ASCE[3]

Abstract: This study derives a semianalytical solution for drawdown distribution during a constant-head test at a partially penetrating well in an unconfined aquifer. The constant-head condition is used to describe the boundary along the screen. In addition, a free-surface condition is used to delineate the upper boundary of the unconfined aquifer. The Laplace-domain solution is then derived using separation of variables and Laplace transform. This solution can be used to identify the aquifer parameters from the data of the constant-head test when integrated with an optimization scheme or to investigate the effects of vertical flow caused by the partially penetrating well and free-surface boundary in an unconfined aquifer. **DOI: 10.1061/(ASCE)HY.1943-7900.0000392.**

CE Database subject headings: Aquifers; Analytical techniques; Wells; Transient flow.

Author keywords: Unconfined aquifer; Semianalytical solution; Partially penetrating well; constant-head test.

Introduction

Aquifer tests, such as constant-head test (CHT) and constant-flux test (CFT), are usually performed to estimate aquifer parameters such as specific storage and hydraulic conductivity. For aquifers with low transmissivity, CHT is more suitable to apply than CFT. The wellbore storage at the pumping well has a large effect on the early drawdown behavior at pumping and observation wells in CFT (Renard 2005). If a CHT is established in a short period of time, the effect of wellbore storage is negligible if the aquifer has low transmissivity and the well radius is small (Chen and Chang 2003).

Many studies have been devoted to the solutions for CHT. Kirkham (1959) derived a steady-state solution for ground-water distribution in a bounded confined aquifer pumped by a partially penetrating well under CHT. They simplified the complexity of the geometry by dividing the model into two different regions. Javandel and Zaghi (1975) considered the ground water in a confined aquifer pumped by a fully penetrating well that is radially extended at the bottom of the aquifer. The procedure used in their study is similar to that in Kirkham (1959), and the steady-state groundwater solution was obtained by separation of variables. Jones et al. (1992) and Jones (1993) discussed the practicality of CHTs on wells completed in low-conductivity glacial till deposits. Mishra and Guyonnet (1992) indicated the operational benefit of CHTs when the total available drawdown is limited by well construction and aquifer characteristics. They developed a method for analyzing observation well response under CHT. Issues involving CHT can be found in the literature (e.g., Uraiet and Raghaven 1980; Chen and Chang 2003; Yeh and Yang 2006; Singh 2007; Wang and Yeh 2008).

Considering a CHT performed in a partially penetrating well, Yang and Yeh (2005) developed a time-domain solution to describe the drawdown in a confined aquifer with a finite-thickness skin. The boundary conditions along the partially penetrating well are represented by a constant-head (first kind) boundary for the screen and a no-flow (second kind) boundary for the casing. They transformed the first-kind boundary along the screen into a second-kind boundary with an unknown flux that is time dependent; therefore, the boundary along the partially penetrating well became uniform. The solution was then solved by the Laplace and finite Fourier cosine transforms. Chang and Yeh (2009) used the methods of dual-series equations and perturbation method to solve the mixed boundary problem for the CHT at a partially penetrating well. Chang and Yeh (2010) further developed an analytical solution for a partially penetrating well with arbitrary location of the well screen under constant-head tests in confined aquifers. However, the aforementioned studies are only applicable for confined aquifers.

For unconfined aquifers, Chen and Chang (2003) developed a well hydraulic theory for CHT performed in a fully penetrating well and established a parameter estimation method. Chang et al. (2010) extended the work of Yang and Yeh (2005) to develop a mathematical model for an unconfined aquifer system while treating the skin as a finite-thickness zone and derived the associated solution for CHT at a partially penetrating well. For other environmental applications, light non-aqueous-phase liquids (LNAPLs) are usually recovered by wells held at constant drawdown (Abdul 1992; Murdoch and Franco 1994), and constant-head pumping is used to control off-site migration of contaminated ground water (Hiller and Levy 1994). At LNAPL contaminant sites, the pollutant forms a pool of LNAPL in the subsurface on top of the water table. In installing a well in unconfined aquifers, therefore, the screen goes from the top of the aquifer.

For CFT in unconfined aquifers, Neuman (1972) presented a new analytical solution for characterizing flow to a fully penetrating well in an unconfined aquifer. He assumed that the drainage above the water table occurs instantaneously. Accounting for the effect of a finite-diameter pumping well, Moench (1997) developed a solution in Laplace domain for the flow to a partially penetrating

[1]Postdoctorate, Institute of Environmental Engineering, National Chiao Tung Univ., Hsinchu, Taiwan. E-mail: rachel.ev91g@nctu.edu.tw

[2]M.S. Student, Institute of Environmental Engineering, National Chiao Tung Univ., Hsinchu, Taiwan. E-mail: sunny0586.ev97g@nctu.edu.tw

[3]Professor, Institute of Environmental Engineering, National Chiao Tung Univ., Hsinchu, Taiwan (corresponding author). E-mail: hdyeh@mail.nctu.edu.tw

Note. This manuscript was submitted on March 9, 2010; approved on December 27, 2010; published online on December 29, 2010. Discussion period open until February 1, 2012; separate discussions must be submitted for individual papers. This paper is part of the ***Journal of Hydraulic Engineering***, Vol. 137, No. 9, September 1, 2011. ©ASCE, ISSN 0733-9429/2011/9-1054–1063/$25.00.

well in unconfined aquifers. Contrary to Neuman's assumption, Moench used the free-surface boundary in Boulton (1955), assuming that the drainage of pores occurs as an exponential function of time in response to a step change in hydraulic head in the aquifer. Tartakovsky and Neuman (2007) presented an analytical solution for drawdown in an unconfined aquifer caused by pumping at a constant rate from a partially penetrating well. They generalized the solution of Neuman (1972, 1974) by accounting for unsaturated flow above the water table and derived the solution from a linearized Richards' equation in which unsaturated hydraulic conductivity and water content are expressed as exponential functions of incremental capillary pressure head relative to its air entry value.

Motivated by the aforementioned research, this paper aims to develop a mathematical model for constant-head pumping from a partially penetrating well in an unconfined aquifer. Without assuming constant-head boundary along the screen as an unknown flux boundary, the system is separated into two different regions, and the solutions are directly obtained by separation of variables and Laplace transform. This new solution can be used to determine the aquifer parameters or to investigate the effects of vertical flow caused by the partially penetrating well and free-surface boundary on the drawdown distribution in unconfined aquifers.

Mathematical Model

Laplace-Domain Solutions

The conceptual model for constant-head pumping in an unconfined aquifer system with a partially penetrating well is illustrated in Fig. 1. The well screen starts from $z = z_l$ with a finite well radius r_w, and the bottom of the screen is sealed. The domain is divided into two different regions. Region 1 is defined by $0 \le r \le r_w$ and $0 \le z \le z_l$ whereas Region 2 is bounded within $r_w \le r < \infty$ and $0 \le z \le \eta$, where η = saturated thickness. The aquifer is assumed to be homogeneous, with infinite extent in the radial direction, and the seepage face in Region 2 is neglected. Under this assumption, the governing equations in terms of drawdown in Regions 1 and 2 can, respectively, be written as

$$K_r\left(\frac{\partial^2 s_1}{\partial r^2}+\frac{1}{r}\frac{\partial s_1}{\partial r}\right)+K_z\frac{\partial^2 s_1}{\partial z^2}=S_s\frac{\partial s_1}{\partial t},\quad 0\le r\le r_w,\qquad 0\le z\le z_l \tag{1}$$

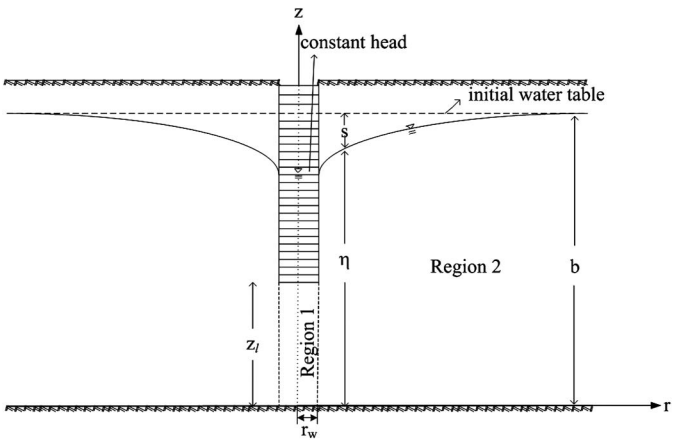

Fig. 1. Schematic of constant-head test in unconfined aquifer with partially penetrating well

and

$$K_r\left(\frac{\partial^2 s_2}{\partial r^2}+\frac{1}{r}\frac{\partial s_2}{\partial r}\right)+K_z\frac{\partial^2 s_2}{\partial z^2}=S_s\frac{\partial s_2}{\partial t},\quad r_w\le r<\infty,\qquad 0\le z\le \eta \tag{2}$$

The subscripts 1 and 2 denote Regions 1 and 2, respectively. The drawdown at distance r from the center of the well and distance z from the bottom of the aquifer at time t is denoted as $s(r,z,t)$, which is equal to $h_0 - h$, where h_0 and h = initial and hydraulic head, respectively. The aquifer has the horizontal hydraulic conductivity K_r, vertical hydraulic conductivity K_z, specific storage S_s, and specific yield S_y. Assuming that the drawdown is small compared with the saturated aquifer thickness η, the boundary at the free surface ($z = \eta$) can be approximated as $z = b$, where b = initial saturated thickness. Therefore, the governing equation for Region 2 can be further expressed as

$$K_r\left(\frac{\partial^2 s_2}{\partial r^2}+\frac{1}{r}\frac{\partial s_2}{\partial r}\right)+K_z\frac{\partial^2 s_2}{\partial z^2}=S_s\frac{\partial s_2}{\partial t},\quad r_w\le r<\infty,\qquad 0\le z\le b \tag{3}$$

The initial condition for saturated thickness $\eta(r,t)$ is equal to b; therefore, the drawdowns are assumed to be zero initially in Regions 1 and 2, that is,

$$s_1(r,z,0)=s_2(r,z,0)=0 \tag{4}$$

The no-flow boundary condition at the bottom of the aquifer for both regions is

$$\left.\frac{\partial s_1(r,z,t)}{\partial z}\right|_{z=0}=\left.\frac{\partial s_2(r,z,t)}{\partial z}\right|_{z=0}=0 \tag{5}$$

The boundary at the top of the Region 1 can also be expressed as

$$\left.\frac{\partial s_1(r,z,t)}{\partial z}\right|_{z=z_l}=0,\qquad 0<r<r_w \tag{6}$$

The nonlinear boundary describing the free surface in Region 2 for the unconfined aquifer can be linearized to the form (Neuman 1972)

$$K_z\left.\frac{\partial s_2(r,z,t)}{\partial z}\right|_{z=b}=-S_y\left.\frac{\partial s_2(r,z,t)}{\partial t}\right|_{z=b} \tag{7}$$

In addition, the boundary at $r = 0$ attributable to symmetry along the center of the well is written as

$$\left.\frac{\partial s_1(r,z,t)}{\partial r}\right|_{r=0}=0,\qquad 0<z<z_1 \tag{8}$$

When r approaches infinity, the boundary condition for Region 2 is

$$s_2(\infty,z,t)=0 \tag{9}$$

The boundary condition specified along the well is

$$s_2(r_w,z,t)=s_w,\qquad z_1<z<b,\qquad t>0 \tag{10}$$

where s_w = constant drawdown in the well at any time.

At the interface between Regions 1 and 2, the continuities of the drawdown and flow rate must be satisfied:

$$s_1(r_w,z,t)=s_2(r_w,z,t),\qquad 0<z<z_l,\qquad t>0 \tag{11}$$

J. Hydraul. Eng. 2011.137:1054-1063.

and

$$\left.\frac{\partial s_1(r,z,t)}{\partial r}\right|_{r=r_w} = \left.\frac{\partial s_2(r,z,t)}{\partial r}\right|_{r=r_w}, \qquad 0 < z < z_l, \qquad t > 0 \tag{12}$$

To express the solutions in dimensionless form, the following dimensionless variables are defined: $s_1^* = s_1/s_w$; $s_2^* = s_2/s_w$; $\sigma = S_y/S_s b$; $\kappa = K_z/K_r$; $\rho = r/r_w$; $\rho_w = r_w/b$; $\alpha_w = \kappa\rho_w^2$; $\alpha = \alpha_w\rho^2$; $\tau = K_r t/S_s r_w^2$; $\zeta = z/b$; and $\zeta_l = z_l/b$, where s_1^* and s_2^* = dimensionless drawdowns for Regions 1 and 2, respectively; σ = ratio of specific yield S_y to the storativity $S_s b$; κ represents the dimensionless conductivity ratio; ρ denotes the dimensionless radial distance; ρ_w = dimensionless radius of the pumping well; α = dimensionless conductivity ratio times the square of the ratio of radial distance r from pumping well to aquifer thickness b; τ refers to the dimensionless time during the test; and ζ and ζ_l = dimensionless vertical distance and the dimensionless distance from the bottom of aquifer to the bottom of the screen, respectively.

Taking the Laplace transform to the dimensionless governing equations of Eqs. (17) and (18) subject to the dimensionless boundary conditions of Eqs. (20)–(27), the Laplace-domain solutions for the dimensionless drawdowns in Regions 1 and 2 are, respectively, as follows:

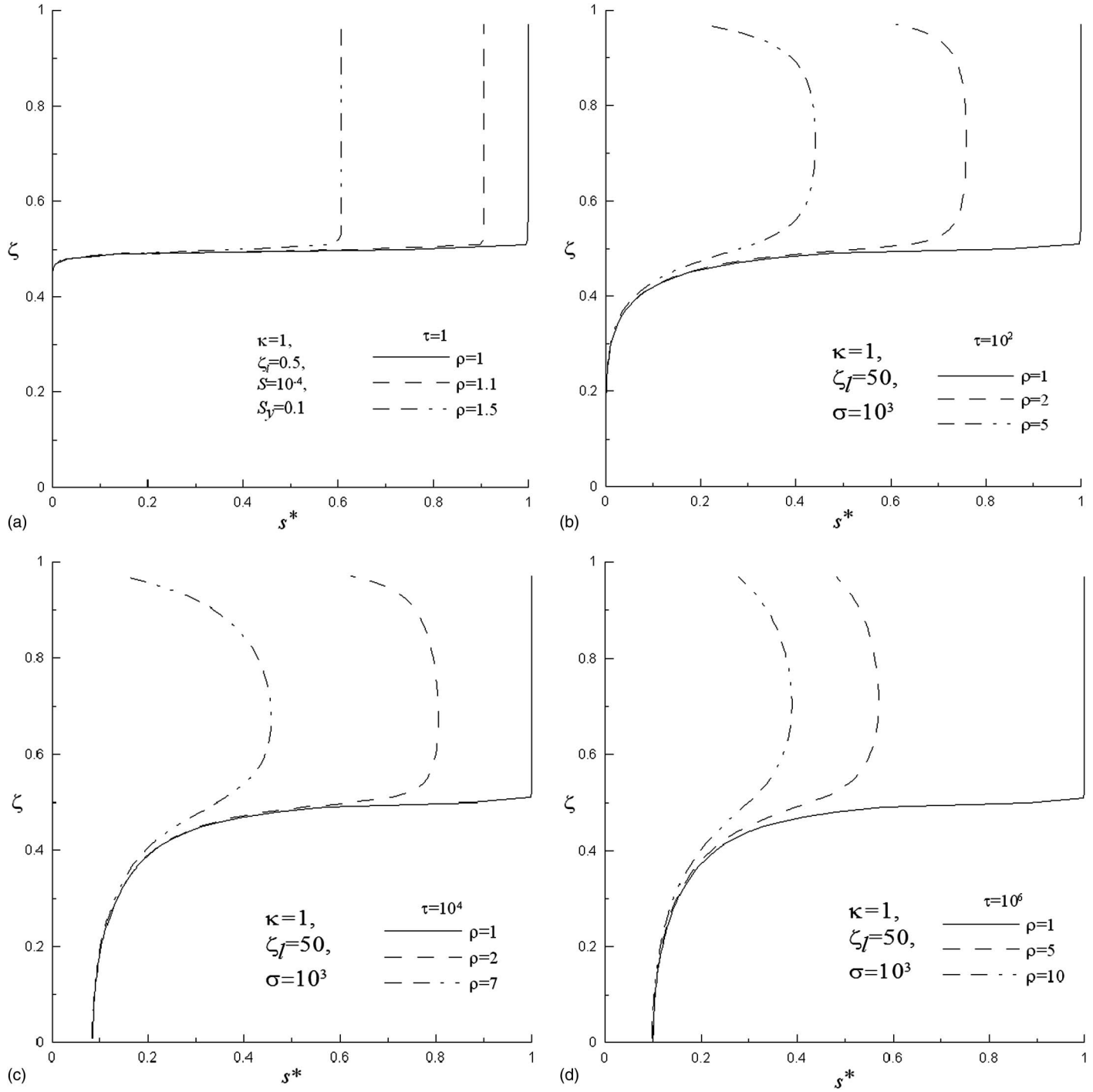

Fig. 2. Dimensionless drawdown distributions at (a) $\tau = 1$, (b) $\tau = 10^2$, (c) $\tau = 10^4$, and (d) $\tau = 10^6$

J. Hydraul. Eng. 2011.137:1054-1063.

$$\tilde{s}_1^*(\rho,\zeta,p)=\sum_{m=0}^{\infty}A'_{1m}(p)\frac{I_0(\sqrt{p+\omega_{1m}}\rho)}{I_0(\sqrt{p+\omega_{1m}})}\cos(\Omega_{1m}\zeta),\qquad t>0 \tag{13}$$

and

$$\tilde{s}_2^*(\rho,\zeta,p)=\sum_{n=0}^{\infty}A'_{2n}(p)\frac{K_0(\sqrt{p+\omega_{2n}}\rho)}{K_0(\sqrt{p+\omega_{2n}})}\cos(\Omega_{2n}\zeta),\qquad t>0 \tag{14}$$

Applying the continuity conditions to Eqs. (13) and (14), the coefficients A'_{1m} and A'_{2n} are respectively obtained as

$$A'_{1m}(p)=-i_{om}\left[\frac{\Omega_{1m}}{\cos(\zeta_l\Omega_{1m})\sin(\zeta_l\Omega_{1m})+\zeta_l\Omega_{1m}}\right]\cdot\sum_{n=0}^{\infty}A'_{2n}(p)k_{0n}\Lambda_{mn} \tag{15}$$

and

$$A'_{2n}(p)=\left[\frac{2\Omega_{2n}}{\sin(2\Omega_{2n})+2\Omega_{2n}}\right]\cdot\sum_{m=0}^{\infty}A'_{1m}(p)\Lambda_{mn}+\frac{4}{p}\left[\frac{\sin(\Omega_{2n})-\sin(\Omega_{2n}\zeta_l)}{\sin(2\Omega_{2n})+2\Omega_{2n}}\right] \tag{16}$$

where p = Laplace variable; and A'_{1m}, A'_{2n}, Ω_{1m}, Ω_{2n},Λ_{mn}, $I_0(\cdot)$, $I_1(\cdot)$, $K_0(\cdot)$, $K_1(\cdot)$, and k_0 are defined in the notation list. The detailed derivations of Eqs. (13) and (14) are given in the appendix.

Fully Penetrating Wells in Unconfined and Confined Aquifers

By setting $\zeta_l=0$ in Eqs. (15) and (16), the drawdown solution of Eq. (13) in Region 1 is equal to zero, and the Laplace-domain solution in Eq. (14) for dimensionless drawdown in Region 2 with fully penetrating wells in unconfined aquifers is exactly the same as the solution given in Chen and Chang [2003, Eq. (7)] when the skin factor S_k equals zero after some algebraic manipulations. Furthermore, by setting $\zeta_l=0$ and $\sigma=0$, the Laplace-domain solution of Eq. (14) in Region 2 can be reduced to the solution in Hantush (1964) for drawdown with a fully penetrating well in confined aquifers.

Results and Discussion

The numerical inversion method given by Stehfest (1970) is adopted for calculating the dimensionless drawdown solutions in Eqs. (13) and (14) for Regions 1 and 2, respectively, in real-time domain. Because there may be nonconvergence issues when evaluating the infinite summations in Eqs. (13) and (14), the Shanks method is applied to accelerate convergence for these infinite summations. This method has been successfully applied to compute the solutions arising in the ground-water area (e.g., Yang and Yeh 2002; Peng et al. 2002).

Fig. 2(a) demonstrates the dimensionless drawdown distributions for the dimensionless distance $\rho=1$, 1.1, and 1.5 at the dimensionless time $\tau=1$, Fig. 2(b) for $\rho=1$, 2, and 5 at $\tau=102$, Fig. 2(c) for $\rho=1$, 2, and 7 at $\tau=10^4$, and Fig. 2(d) for $\rho=1$, 5, and 7 at $\tau=10^6$. The aquifer parameters used in these figures are as follows: $\kappa=1$, $\sigma=10^{-3}$, and $\zeta_l=0.5$. These figures show that the dimensionless drawdown at $\rho=1$ matches the boundary condition of the wellbore at different time periods. The dimensionless drawdown decreases with increasing ρ at $\tau=1$, 102, 104, and 106. In addition, it is apparent that vertical flows occur at the water table because of the free-surface boundary, as shown in Figs. 2(b)–2(d).

Fig. 3 is plotted to examine the effect σ (i.e., S_y/S_sb) of Region 2 on the dimensionless drawdown during CHT. This figure shows the response of dimensionless drawdown in a 100-m-thick aquifer at $\rho=50$, $\kappa=1$, $\zeta=0.75$, and $\zeta_l=0.5$ for σ ranging from 0 to 3×10^3. The dimensionless drawdown decreases with increasing σ. The typical three-stage drawdown patterns can be observed. The water releases from the elastic behavior of the aquifer formation at an early time, i.e., the first stage. During the second stage at moderate times, the gravity drainage almost stabilizes the water table. Finally, the effect of vertical flow vanishes at late times, and the flow behaves like the first stage again. Fig. 3 shows that the larger σ is, the longer the delayed yield stage will be, perhaps because a larger σ supply more water from the drainage. If $\sigma=0$, the top boundary represented by Eq. (7) becomes the no-flow condition, and the aquifer can therefore be considered as confined.

Fig. 4 illustrates that the distributions of the dimensionless drawdown at the well screen extends from $\zeta=\zeta_l$ to $\zeta=1$ in Region 2 when $\tau=10^6$. This figure shows that the dimensionless drawdown increases with the length of well screen. In addition, large slopes of the drawdown distribution curves occur near the free-surface boundary and the edge of the screen. Therefore, vertical ground-water flows are obviously large at these two areas.

The response of dimensionless drawdown versus dimensionless time at different observed locations is plotted in Fig. 5 for $\rho=10$ and 100 with $\kappa=1$ and $\zeta_l=0.25$. The σ is zero for a confined aquifer, and there is no vertical flow [Fig. 5(a)]. On the other hand, the vertical flow is apparent at moderate times for different radial distances [Fig. 5(b)] when $\sigma=10^3$. Figs. 6(a) and 6(b) illustrates the spatial flow pattern for $\sigma=0$ and 10^3 at $\tau=10^4$ with the same parameter values as those in Fig. 5. Apparently, the vertical flow occurs only near the bottom edge of the well screen when the aquifer is confined. However, for unconfined aquifers, the flow at free surface is almost vertical, and obvious vertical flows occur near both the top and bottom edges of the well. It demonstrates that the vertical flow in the unconfined system is induced not only by the effect of partial penetration but also the effect of free-surface boundary.

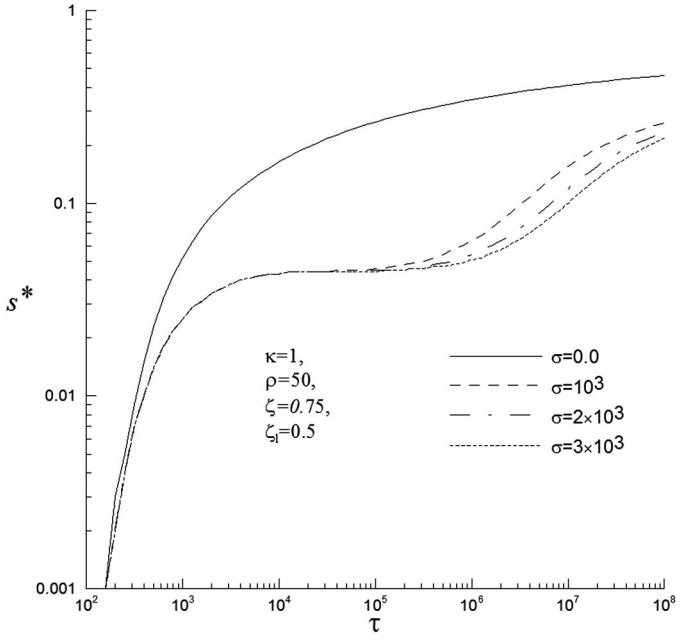

Fig. 3. Effect of σ on dimensionless drawdown during CHT

J. Hydraul. Eng. 2011.137:1054-1063.

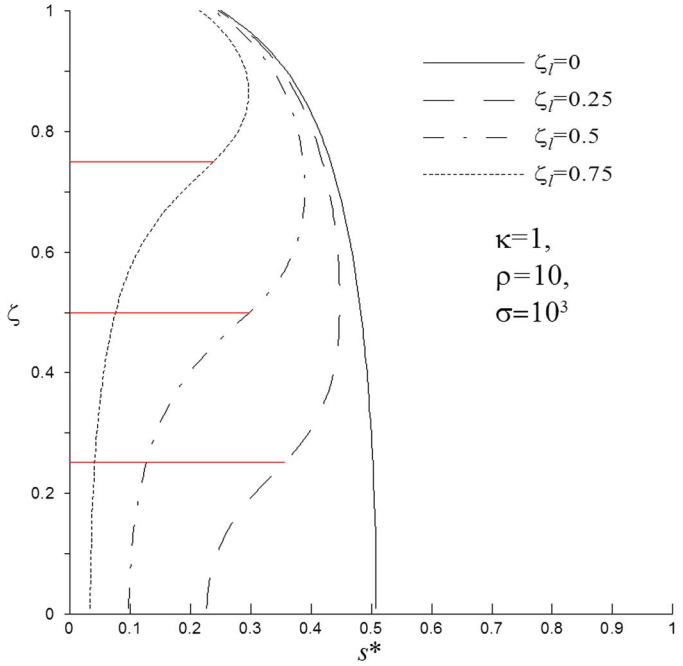

Fig. 4. Dimensionless drawdown distributions at well screen extended from $\zeta = \zeta_l$ to $\zeta = 1$ in Region 2

Fig. 7 demonstrates the effect of the conductivity ratio $\kappa(= K_z/K_r)$ on the dimensionless drawdown during CHT. The vertical axis represents the dimensionless drawdown, and the horizontal axis represents the dimensionless time. The κ ranges from 10^{-2} to 1 with $K_r = 10^{-4}$ m/min, $\sigma = 10^3$, and $\zeta_l = 0.5$. The dimensionless drawdown decreases with increasing κ, indicating that the vertical flow from delayed gravity drainage becomes large for greater κ. Fig. 8 illustrates the effect of the well radius on drawdown distribution in a 10-m-thick aquifer. The considered ρ_w well radii are 0.1, 0.01, and 0.001 m with $\sigma = 10^3$, $\zeta = 0.75$, $\zeta_l = 0.5$, and $\kappa = 1$. Drawdown is calculated at the dimensionless distances of 3.16, 10, or 31.6 from the pumping well for $\alpha = 10^{-1}$, 1, and 101, respectively. The drawdown decreases with increasing distance from the pumping well for different ρ_w, as demonstrated in Fig. 2. The drawdown increases with ρ_w for different values of α, indicating that the well radius has significant effect on the drawdown distribution. The effect of α on drawdown in the aquifer at $\zeta = 0$ when the well is fully ($\zeta_l = 0$) and partially penetrating ($\zeta_l = 0.8$) is plotted in Fig. 9 for $\sigma = 10^3$ and $\kappa = 1$. The drawdown difference between the cases of full penetration and partial penetration decreases with increasing α. It is reasonable that $\alpha^{1/2}$ is directly proportional to the radial distance from the pumping well when the aquifer is isotropic, and the partial penetration effect vanishes when the radial distance becomes large. Because $r = \alpha^{1/2} b/\sqrt{\kappa}$, this proves that the radial distance influenced by the partial penetration in an unconfined aquifer under CHT is proportional to the aquifer thickness, as do the results from Hantush (1964) for a confined aquifer under CFT.

The error of estimated dimensionless drawdown along the screen calculated from Eqs. (13) and (14) for different number of terms of the infinite series and Shanks method is demonstrated in Fig. 10. As illustrated in this figure, the error decreases with increasing number of terms used in calculating the infinite series in the solution, and the largest error occurs at the edges of the screen. The largest errors are -0.179 when $n = m = 100$; 9.72×10^{-2} when $n = m = 200$; -4.22×10^{-2} when $n = m = 500$; 2.02×10^{-2} when $n = m = 1{,}000$; and 5.64×10^{-4} when applying Shanks method. On the other hand, the smallest errors are -9.61×10^{-3} when $n = m = 100$; 4.61×10^{-3} when $n = m = 200$; -1.91×10^{-4} when $n = m = 500$; 9.35×10^{-4} when $n = m = 1{,}000$; and -6.18×10^{-10} when applying Shanks method. These results indicate that the Shanks method can be applied to effectively accelerate convergence for the infinite summations in dimensionless drawdown in Eqs. (13) and (14).

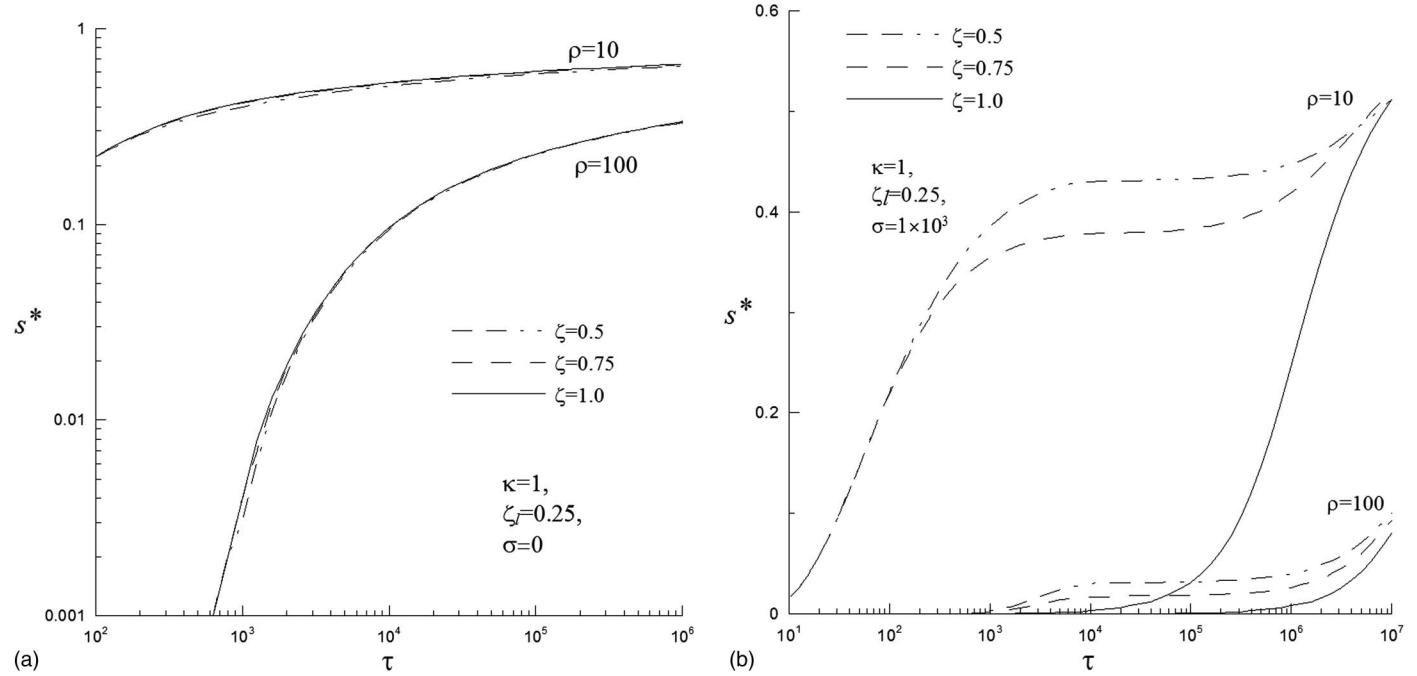

Fig. 5. Relationship for dimensionless drawdown versus dimensionless time with $\zeta = 0.5$, 0.75, and 1.0 at $\rho = 10$ or 100 for (a) $\sigma = 0$ and (b) $\sigma = 10^3$

J. Hydraul. Eng. 2011.137:1054-1063.

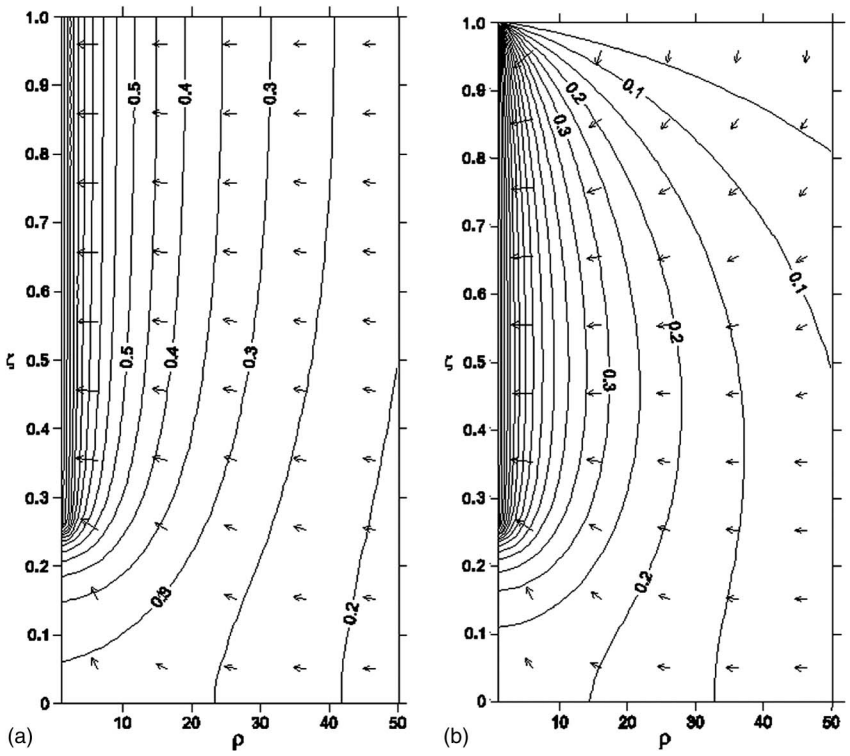

Fig. 6. Spatial flow pattern in unconfined aquifer with partially penetrating well for $\kappa = 1$, $\zeta_l = 0.25$ at $\tau = 10^4$ when (a) $\sigma = 0$ and (b) $\sigma = 10^3$

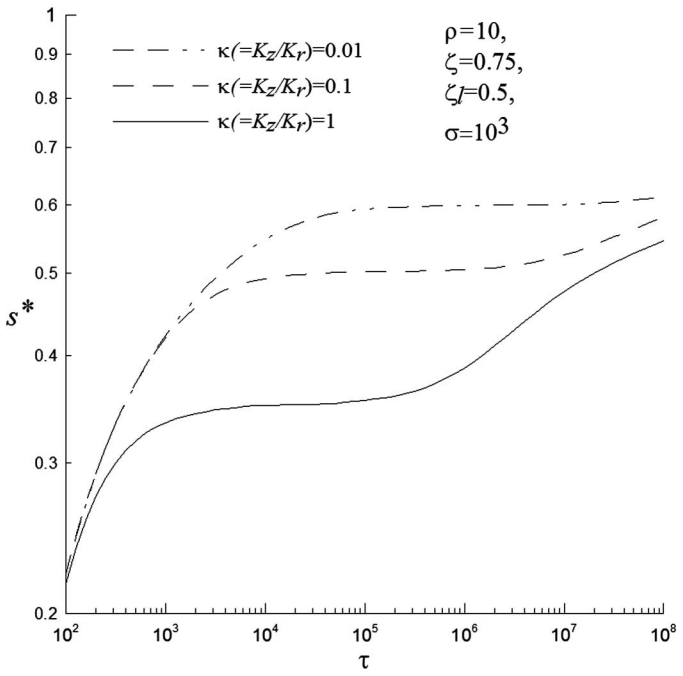

Fig. 7. Effect of conductivity ratio (κ) of Region 2 on dimensionless drawdown during CHT

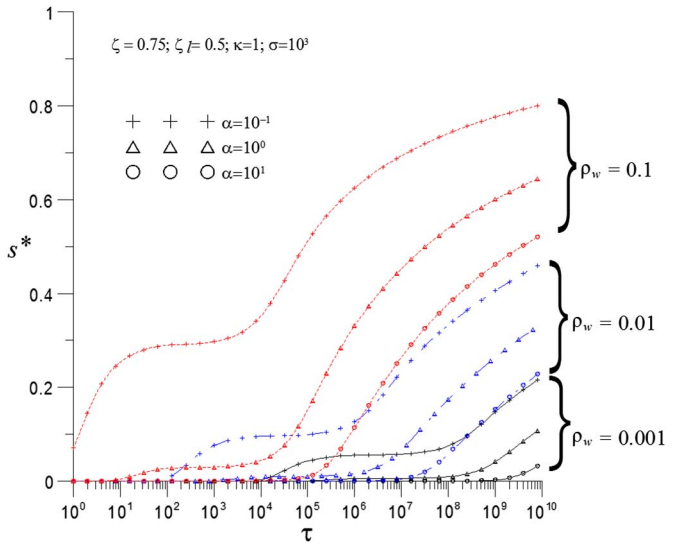

Fig. 8. Drawdown distribution for well with three different values of dimensionless well radii ($\rho_w = 0.1$, 0.01, and 0.001) with $\sigma = 10^3$, $\zeta = 0.75$, $\zeta_l = 0.5$, and $\kappa = 1$

Concluding Remarks

A semianalytical solution of the drawdown distribution is developed for CHT performed in an unconfined aquifer with a partially penetrating well. The Laplace transforms and the method of separation of variables are used to derive the transient drawdown in the Laplace domain for CHT. The Stehfest method is used to invert the solutions in time domain, and the Shanks method is applied to accelerate convergence in evaluating the infinite summations in the solution.

Large slopes of the drawdown distribution curves can be observed near the free-surface boundary and the edge of the screen, which indicates that the vertical ground-water flows occur at these two areas. The dimensionless drawdown decreases with increasing σ but increases with the length of well screen. For different ρ_w, the drawdown decreases with the increase of radial distance from the pumping well, and it may produce a large error in drawdown if the radius of the pumping well is assumed infinitesimal.

J. Hydraul. Eng. 2011.137:1054-1063.

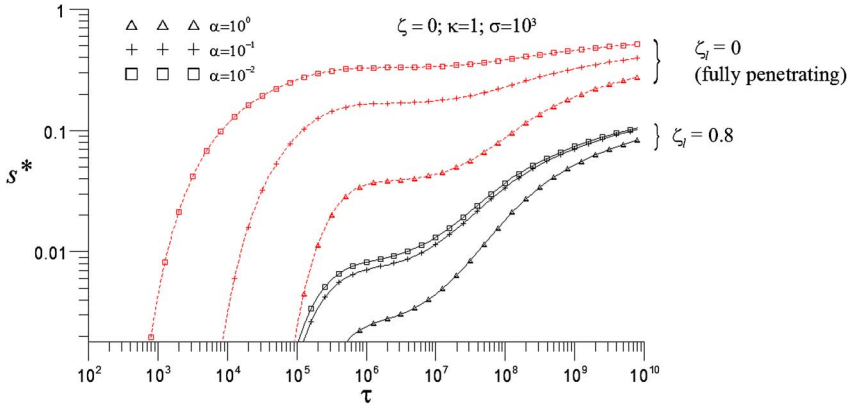

Fig. 9. Effect of α on drawdown in 100-m-thick aquifer when $\sigma = 10^3$, $\kappa = 1$ at $\zeta = 0$ for $\alpha = 10^0$, 10^{-1}, and 10^{-2}

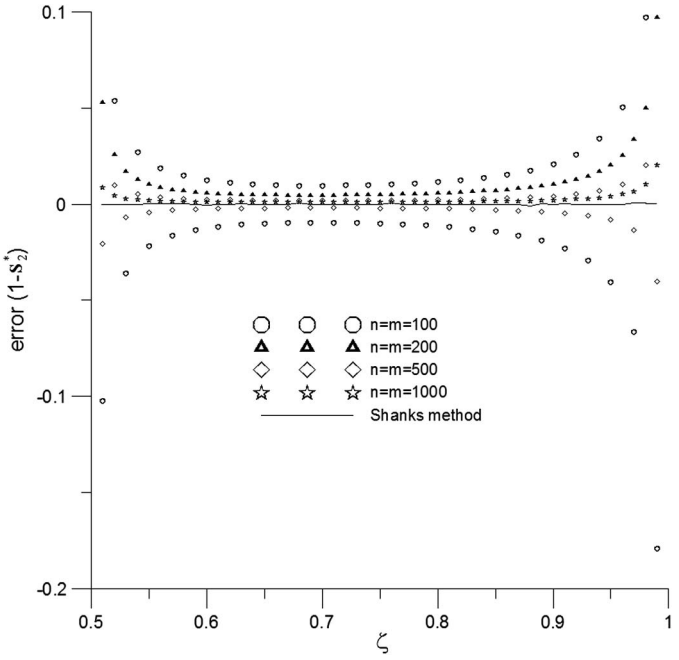

Fig. 10. Error of estimated dimensionless drawdown along screen calculated from Eqs. (13) and (14) for different number of terms of infinite series and Shanks method

The present solution can serve as an invaluable tool to explore the effects of hydraulic parameters on flow behavior in unconfined aquifers. In addition, it can reduce the solution for a fully penetrating well in confined or unconfined aquifers under CHT.

Appendix

The dimensionless governing equations of Eqs. (1) and (3) can be expressed as

$$\frac{\partial^2 s_1^*}{\partial \rho^2} + \frac{1}{\rho}\frac{\partial s_1^*}{\partial \rho} + \alpha_w \frac{\partial^2 s_1^*}{\partial \zeta^2} = \frac{\partial s_1^*}{\partial \tau}, \qquad 0 \le \rho \le 1, \qquad 0 \le \zeta \le \zeta_l \tag{17}$$

and

$$\frac{\partial^2 s_2^*}{\partial \rho^2} + \frac{1}{\rho}\frac{\partial s_2^*}{\partial \rho} + \alpha_w \frac{\partial^2 s_2^*}{\partial \zeta^2} = \frac{\partial s_2^*}{\partial \tau}, \qquad 1 \le \rho < \infty, \qquad 0 \le \zeta \le 1 \tag{18}$$

The dimensionless initial conditions for Regions 1 and 2 are

$$s_1^*(\rho, \zeta, 0) = s_2^*(\rho, \zeta, 0) = 0 \tag{19}$$

and the boundary conditions at the bottom and top of the aquifer for Regions 1 and 2 in terms of dimensionless form can be written as

$$\left.\frac{\partial s_1^*(\rho, \zeta, \tau)}{\partial \zeta}\right|_{\zeta=0} = \left.\frac{\partial s_2^*(\rho, \zeta, \tau)}{\partial \zeta}\right|_{\zeta=0} = 0 \tag{20}$$

$$\left.\frac{\partial s_1^*(\rho, \zeta, \tau)}{\partial \zeta}\right|_{\zeta=\zeta_l} = 0, \qquad 0 < \rho < 1 \tag{21}$$

and

$$\left.\frac{\partial s_2^*(\rho, \zeta, \tau)}{\partial \zeta}\right|_{\zeta=1} = -\frac{\sigma}{\alpha_w}\left.\frac{\partial s_2^*(\rho, \zeta, \tau)}{\partial \tau}\right|_{\zeta=1}, \qquad 1 \le \rho < \infty \tag{22}$$

The dimensionless boundary conditions at $\rho = 0$ and infinity are respectively written as

$$\frac{\partial s_1^*(0, \zeta, \tau)}{\partial \rho} = 0, \qquad 0 < \zeta < \zeta_l \tag{23}$$

$$s_2^*(\infty, \zeta, \tau) = 0 \tag{24}$$

The dimensionless boundary condition along the screen is expressed as

$$s_2^*(1, \zeta, \tau) = 1, \qquad \zeta_l < \zeta < 1, \qquad \tau > 0 \tag{25}$$

In dimensionless form, continuity conditions become

$$s_1^*(1, \zeta, \tau) = s_2^*(1, \zeta, \tau), \qquad 0 < \zeta < \zeta_l, \qquad \tau > 0 \tag{26}$$

and

$$\left.\frac{\partial s_1^*(\rho, \zeta, \tau)}{\partial \rho}\right|_{\rho=1} = \left.\frac{\partial s_2^*(\rho, \zeta, \tau)}{\partial \rho}\right|_{\rho=1}, \qquad 0 < \zeta < \zeta_l, \qquad \tau > 0 \tag{27}$$

The solution for the dimensionless drawdown solutions can be obtained by taking Laplace transforms of governing equations Eqs. (17) and (18) using the initial condition (19), and the results are

J. Hydraul. Eng. 2011.137:1054-1063.

$$\frac{\partial^2 \tilde{s}_1^*}{\partial \rho^2} + \frac{1}{\rho}\frac{\partial \tilde{s}_1^*}{\partial \rho} + \alpha_w \frac{\partial^2 \tilde{s}_1^*}{\partial \zeta^2} = p\tilde{s}_1^*, \qquad 0 \le \rho \le 1, \qquad 0 \le \zeta \le \zeta_l \tag{28}$$

and

$$\frac{\partial^2 \tilde{s}_2^*}{\partial \rho^2} + \frac{1}{\rho}\frac{\partial \tilde{s}_2^*}{\partial \rho} + \alpha_w \frac{\partial^2 \tilde{s}_2^*}{\partial \zeta^2} = p\tilde{s}_2^*, \qquad 1 \le \rho < \infty, \qquad 0 \le \zeta \le 1 \tag{29}$$

The transformed boundary conditions at the bottom and top of the aquifer for Regions 1 and 2 can be written as

$$\left.\frac{\partial \tilde{s}_1^*(\rho,\zeta,p)}{\partial \zeta}\right|_{\zeta=0} = \left.\frac{\partial \tilde{s}_2^*(\rho,\zeta,p)}{\partial \zeta}\right|_{\zeta=0} = 0 \tag{30}$$

$$\left.\frac{\partial \tilde{s}_1^*(\rho,\zeta,p)}{\partial \zeta}\right|_{\zeta=\zeta_l} = 0, \qquad 0 < \rho < 1 \tag{31}$$

and

$$\left.\frac{\partial \tilde{s}_2^*(\rho,\zeta,p)}{\partial \zeta}\right|_{\zeta=1} = -\frac{\sigma}{\alpha_w}\cdot p \cdot \tilde{s}_2^*(\rho,\zeta=1,p) \tag{32}$$

Likewise, the transformed boundary conditions at $\rho = 0$ and ∞ are

$$\frac{\partial \tilde{s}_1^*(0,\zeta,p)}{\partial \rho} = 0, \qquad 0 < \zeta < \zeta_l \tag{33}$$

and

$$\tilde{s}_2^*(\infty,\zeta,p) = 0 \tag{34}$$

After taking the Laplace transform, the boundary condition along the well screen is

$$\tilde{s}_2^*(1,\zeta,p) = \frac{1}{p}, \qquad \zeta_l < \zeta < 1, \qquad \tau > 0 \tag{35}$$

and continuity conditions become

$$\tilde{s}_2^*(1,\zeta,p) = \tilde{s}_1^*(1,\zeta,p), \qquad 0 < \zeta < \zeta_l \tag{36}$$

and

$$\left.\frac{\partial \tilde{s}_1^*(\rho,\zeta,p)}{\partial \rho}\right|_{\rho=1} = \left.\frac{\partial \tilde{s}_2^*(\rho,\zeta,p)}{\partial \rho}\right|_{\rho=1}, \qquad 0 < \zeta < \zeta_l \tag{37}$$

Assume that $\tilde{s}_1^*$ and $\tilde{s}_2^*$ are the product of two distinct functions, i.e., $\tilde{s}_1^*(\rho,\zeta,p) = F_1(\rho,p)G_1(\zeta,p)$ and $\tilde{s}_2^*(\rho,\zeta,p) = F_2(\rho,p)G_2(\zeta,p)$, respectively. Eqs. (12) and (13) can be respectively transformed as

$$G_1\frac{\partial^2 F_1}{\partial \rho^2} + G_1\frac{1}{\rho}\frac{\partial F_1}{\partial \rho} + \alpha_w F_1\frac{\partial^2 G_1}{\partial \zeta^2} = pF_1G_1 \tag{38}$$

and

$$G_2\frac{\partial^2 F_2}{\partial \rho^2} + G_2\frac{1}{\rho}\frac{\partial F_2}{\partial \rho} + \alpha_w F_2\frac{\partial^2 G_2}{\partial \zeta^2} = pF_2G_2 \tag{39}$$

Dividing Eqs. (38) and (39) by F_1G_1 and F_2G_2, respectively, Eqs. (38) and (39) can then be separated into the following two systems of ordinary differential equations after some arrangements:

$$\frac{\partial^2 G_1}{\partial \zeta^2} + \frac{\omega_{1m}}{\alpha_w}G_1 = 0 \tag{40}$$

$$\frac{\partial^2 F_1}{\partial \rho^2} + \frac{1}{\rho}\frac{\partial F_1}{\partial \rho} - [p + \omega_{1m}]F_1 = 0 \tag{41}$$

and

$$\frac{\partial^2 G_2}{\partial \zeta^2} + \frac{\omega_{2n}}{\alpha_w}G_2 = 0 \tag{42}$$

$$\frac{\partial^2 F_2}{\partial \rho^2} + \frac{1}{\rho}\frac{\partial F_2}{\partial \rho} - [p + \omega_{2n}]F_2 = 0 \tag{43}$$

where ω_{1m} and ω_{1n} = separation constants.

The solutions of Eqs. (40) and (42) subject to the boundary in Eq. (30) are, respectively, as follows:

$$G_1(\zeta,p) = a_{1m}(p)\cos(\Omega_{1m}\zeta) \tag{44}$$

and

$$G_2(\zeta,p) = a_{2n}(p)\cos(\Omega_{2n}\zeta) \tag{45}$$

where $\Omega_{1m} = \sqrt{\omega_{1m}/\alpha_w}$; $\Omega_{2n} = \sqrt{\omega_{2n}/\alpha_w}$; and $a_{1m}(p)$ and $a_{2n}(p)$ = constants with respect to ζ. In addition, substituting Eq. (44) into Eq. (31) yields the following equation:

$$\sin(\Omega_{1m}\zeta_l) = 0 \tag{46}$$

The eigenvalues Ω_{1m} in Eq. (44) can then determined by solving Eq. (46) and results in

$$\Omega_{1m} = \frac{m\pi}{\zeta_l}, \qquad m = 0, 1, 2, \ldots \tag{47}$$

Similarly, substituting Eq. (45) into Eq. (32) gives the following equation:

$$\Omega_{2n}\sin(\Omega_{2n}) = \frac{\sigma}{\alpha_w}p\cos(\Omega_{2n}), \qquad n = 0, 1, 2, \ldots \tag{48}$$

Eq. (48) can be solved to obtain the eigenvalues Ω_{2n} in Eq. (45).

The solutions of Eqs. (41) and (43) are, respectively, as follows:

$$F_1(\rho,p) = c_{1m}(p)I_0(\sqrt{p+\omega_{1m}}\rho) \tag{49}$$

and

$$F_2(\rho,p) = d_{2n}(p)K_0(\sqrt{p+\omega_{2n}}\rho) \tag{50}$$

where $c_{1m}(p)$ and $d_{2n}(p)$ = constants. Note that $d_{1m}(p)$ and $c_{2n}(p)$ equal zero when using the boundary conditions of Eqs. (33) and (34), respectively.

The product of Eqs. (44) and (49) gives the general solution of Eq. (36) as

$$\tilde{s}_{1m}^*(\rho,\zeta,p) = A_{1m}(p)I_0(\sqrt{p+\omega_{1m}}\rho)\cos(\Omega_{1m}\zeta), \quad m = 0, 1, 2, \ldots \tag{51}$$

where $A_{1m}(p)$ = product of $a_{1m}(p)$ and $c_{1m}(p)$. On the other hand, the product of Eqs. (35) and (50) forms the general solution of Eq. (39) as

$$\tilde{s}_{2n}^*(\rho,\zeta,p) = A_{2n}(p)K_0(\sqrt{p+\omega_{2n}}\rho)\cos(\Omega_{2n}\zeta) \qquad n = 0, 1, 2, \ldots \tag{52}$$

where $A_{2n}(p)$ = product of $a_{2n}(p)$ and $d_{2n}(p)$. Accordingly, the linear combination of all solutions of m yields the complete solution for $\tilde{s}_1^*(\rho,\zeta,p)$

$$\tilde{s}_1^*(\rho,\zeta,p) = \sum_{m=0}^{\infty} A_{1m}(p)I_0(\sqrt{p+\omega_{1m}}\rho)\cos(\Omega_{1m}\zeta) \tag{53}$$

J. Hydraul. Eng. 2011.137:1054-1063.

Similarly, the complete solution for $\tilde{s}_2^*(\rho,\zeta,p)$ can be obtained as

$$\tilde{s}_2^*(\rho,\zeta,p)=\sum_{n=0}^{\infty}A_{2n}(p)K_0(\sqrt{p+\omega_{2n}}\rho)\cos(\Omega_{2n}\zeta) \tag{54}$$

The coefficients $A_{1m}(p)$ and $A_{2n}(p)$ are unknowns at this stage and can be solved from the following equation obtained by substituting Eqs. (53) and (54) into Eqs. (35) and (36), respectively, as

$$\sum_{n=0}^{\infty}A_{2n}(p)K_0(\sqrt{p+\omega_{2n}})\cos(\Omega_{2n}\zeta)=\frac{1}{p},\qquad \zeta_l<\zeta<1 \tag{55}$$

and

$$\sum_{m=0}^{\infty}A_{1m}(p)I_0(\sqrt{p+\omega_{1m}})\cos(\Omega_{1m}\zeta)=\sum_{n=0}^{\infty}A_{2n}(p)K_0(\sqrt{p+\omega_{2n}})\cos(\Omega_{2n}\zeta),\qquad 0<\zeta<\zeta_l \tag{56}$$

Eqs. (55) and (56) are organized and expressed as

$$\sum_{n=0}^{\infty}A_{2n}(p)K_0(\sqrt{p+\omega_{2n}})\cos(\Omega_{2n}\zeta)=\sum_{m=0}^{\infty}A_{1m}(p)I_0(\sqrt{p+\omega_{1m}})\cos(\Omega_{1m}\zeta),\qquad 0<\zeta<\zeta_l$$
$$=\frac{1}{p},\qquad \zeta_l<\zeta<1 \tag{57}$$

To obtain concise solutions, $A'_{2n}(p)=A_{2n}(p)K_0(\sqrt{p+\omega_{2n}})$ and $A'_{1m}(p)=A_{1m}(p)I_0(\sqrt{p+\omega_{1m}})$ are further defined, and Eq. (57) can be rewritten as

$$\sum_{n=0}^{\infty}A'_{2n}(p)\cos(\Omega_{2n}\zeta)=f(\zeta),\qquad 0<\zeta<1 \tag{58}$$

where

$$f(\zeta)=\sum_{m=0}^{\infty}A'_{1m}(p)\cos(\Omega_{1m}\zeta),\qquad 0<\zeta<\zeta_l$$
$$=\frac{1}{p},\qquad \zeta_1<\zeta<1 \tag{59}$$

The term on the left-hand side (LHS) of Eq. (58) is a half-range Fourier cosine series of the function on the right-hand side (RHS) for the region $0<\zeta<1$. The coefficient $A'_{2n}(p)$ can then be obtained from the properties of the Fourier series as

$$A'_{2n}(p)=\frac{\int_0^1\cos(\Omega_{2n}\zeta)f(\zeta)d\zeta}{\int_0^1\cos^2(\Omega_{2n}\zeta)d\zeta} \tag{60}$$

Carrying out the integration in Eq. (60) and simplifying the result yields the coefficient $A'_{2n}(p)$ as expressed in Eq. (16).

Similarly, substituting Eqs. (53) and (54) into Eq. (37), one can obtain

$$\sum_{m=0}^{\infty}A'_{1m}(p)\sqrt{p+\omega_{1m}}\frac{I_1(\sqrt{p+\omega_{1m}})}{I_0(\sqrt{p+\omega_{1m}})}\cos(\Omega_{1m}\zeta)=-\sum_{n=0}^{\infty}A'_{2n}(p)\sqrt{p+\omega_{2n}}\frac{K_1(\sqrt{p+\omega_{2n}})}{K_0(\sqrt{p+\omega_{2n}})}\cos(\Omega_{2n}\zeta), \tag{61}$$
$$0<\zeta<\zeta_l$$

From Eq. (61), the coefficient $A'_{1m}(p)$ can be determined as Eq. (15).

Accordingly, based on the coefficients $A'_{1m}(p)$ and $A'_{2n}(p)$, the complete solution for $\tilde{s}_1^*$ and $\tilde{s}_2^*$ can be obtained as Eqs. (13) and (14), respectively.

Notation

The following symbols are used in this paper:

$A'_{1m}=A_{1m}(p)I_0(\sqrt{p+\omega_{1m}})$;
$A'_{2n}=A_{2n}(p)K_0(\sqrt{p+\omega_{2n}})$;
$s_1^*=s_1/s_w$;
$s_2^*=s_2/s_w$;
$I_0(\cdot)$ = modified Bessel function of first kind of order 0;
$I_1(\cdot)$ = modified Bessel function of first kind of order 1;
$i_{0m}=I_0(\sqrt{p+\omega_{1m}})/[\sqrt{p+\omega_{1m}}\cdot I_1(\sqrt{p+\omega_{1m}})]$
$K_0(\cdot)$ = modified Bessel function of second kind of order 0;
$K_1(\cdot)$ = modified Bessel function of second kind of order 1;
$k_{0n}=[\sqrt{p+\omega_{2n}}\cdot K_1(\sqrt{p+\omega_{2n}})]/K_0(\sqrt{p+\omega_{2n}})$;
$\beta=b/r_w$;
$\zeta=z/b$;
$\zeta_l=z_l/b$;
$\kappa=K_z/K_r$;
$\Lambda_{mn}=\{\sin[(\Omega_{1m}+\Omega_{2n})\zeta_l]/(\Omega_{1m}+\Omega_{2n})\}+\{\sin[(\Omega_{1m}-\Omega_{2n})\zeta_l]/(\Omega_{1m}-\Omega_{2n})\}$;
$\rho=r/r_w$;
$\tau=K_rt/S_sr_w^2$;
$\Omega_{1m}=\beta\sqrt{\omega_{1m}/k}$; and
$\Omega_{2n}=\beta\sqrt{\omega_{2n}/k}$.

Acknowledgments

Research leading to this work has been partially supported by the grants from Taiwan National Science Council under the contract numbers NSC 96-2221-E-009-087-MY3, NSC 98-3114-E-007-015, and NSC 99-NU-E-009-001.

References

Abdul, A. S. (1992). "A new pumping strategy for petroleum product recovery from contaminated hydrogeologic systems: Laboratory and field evaluations." *Ground Water Monit. Rem.*, 12(1), 105–114.

Boulton, N. S. (1955). "Unsteady radial flow to a pumped well allowing for delayed yield from storage." *Gen. Assera. Rome, Tome II, Int. Assoc. Sci. Hydrol. Publ.*, 37, 472–477.

Chang, Y. C., and Yeh, H. D. (2009). "New solutions to the constant-head test performed at a partially penetrating well." *J. Hydrol.*, 369(1–2), 90–97.

Chang, Y. C., and Yeh, H. D. (2010). "A new analytical solution solved by triple series equations method for constant-head tests in confined aquifers." *Adv. Water Resour.*, 33(6), 640–651.

Chang, Y. C., Yeh, H. D., and Chen, G. Y. (2010). "Transient solution for radial two-zone flow in unconfined aquifers under constant-head test." *Hydrol. Processes*, 24(11), 1496–1503.

Chen, C. S., and Chang, C. C. (2003). "Well hydraulics theory and data analysis of the constant head test in an unconfined aquifer with the skin effect." *Water Resour. Res.*, 39(5), 1121–1135.

Hantush, M. S. (1964). "Hydraulics of wells." *Advances in hydroscience*, Vol. 1, V. T. Chow, ed., Academic, San Diego, 281–432.

J. Hydraul. Eng. 2011.137:1054-1063.

Hiller, C. K., and Levy, B. S. (1994). "Estimation of aquifer diffusivity from analysis of constant-head pumping test data." *Ground Water*, 32(1), 47–52.

Javandel, I., and Zaghi, N. (1975). "Analysis of flow to an extended fully penetrating well." *Water Resour. Res.*, 11(1), 159–164.

Jones, L. (1993). "A comparison of pumping and slug tests for estimating the hydraulic conductivity of unweathered Wisconsin age till in Iowa." *Ground Water*, 31(6), 896–904.

Jones, L., Lemar, T., and Tsai, C. T. (1992). "Results of two pumping tests in Wisconsin age weathered till in Iowa." *Ground Water*, 30(4), 529–538.

Kirkham, D. (1959). "Exact theory of flow into a partially penetrating well." *J. Geophys. Res.*, 64(9), 1317–1327.

Mishra, S., and Guyonnet, D. (1992). "Analysis of observation-well response during constant-head testing." *Ground Water*, 30(4), 523–528.

Moench, A. F. (1997). "Flow to a well of finite diameter in a homogeneous, anisotropic water table aquifer." *Water Resour. Res.*, 33(6), 1397–1407.

Murdoch, L. D., and Franco, J. (1994). "The analysis of constant drawdown wells using instantaneous source functions." *Water Resour. Res.*, 30(1), 117–127.

Neuman, S. P. (1972). "Theory of flow in unconfined aquifers considering delayed response of the water table." *Water Resour. Res.*, 8(4), 1031–1045.

Neuman, S. P. (1974). "Effects of partial penetration on flow in unconfined aquifers considering delayed aquifer response." *Water Resour. Res.*, 10(2), 303–312.

Peng, H. Y., Yeh, H. D., and Yang, S. Y. (2002). "Improved numerical evaluation of the radial groundwater flow equation." *Adv. Water Resour.*, 25(6), 663–675.

Renard, P. (2005). "Approximate discharge for constant head test with recharging boundary." *Ground Water*, 43(3), 439–442.

Singh, S. K. (2007). "Simple approximation of well function for constant drawdown variable discharge artesian wells." *J. Irrig. Drain. Eng.*, 133(3), 282–285.

Stehfest, H. (1970). "Numerical inversion of Laplace transforms." *Commun. ACM*, 13(1), 47–49.

Tartakovsky, G. D., and Neuman, S. P. (2007). "Three-dimensional saturated-unsaturated flow with axial symmetry to a partially penetrating well in a compressible unconfined aquifer." *Water Resour. Res.*, 43, W01410, 10.1029/2006WR005153.

Uraiet, A. A., and Raghavan, R. (1980). "Unsteady flow to a well producing at a constant pressure." *J. Pet. Technol.*, 32(10), 1803–1812.

Wang, C. T., and Yeh, H. D. (2008). "Obtaining the steady-state drawdown solutions of constant-head and constant-flux tests." *Hydrol. Processes*, 22(17), 3456–3461, 10.1002/hyp.6950.

Yang, S. Y., and Yeh, H. D. (2002). "Solution for flow rates across the wellbore in a two-zone confined aquifer." *J. Hydraul. Eng.*, 128(2), 175–183.

Yang, S. Y., and Yeh, H. D. (2005). "Laplace-domain solutions for radial two-zone flow equations under the conditions of constant-head and partially penetrating well." *J. Hydraul. Eng.*, 131(3), 209–216.

Yeh, H. D., and Yang, S. Y. (2006). "A novel analytical solution for constant-head test in a patchy aquifer." *Int. J. Numer. Anal. Methods Geomech.*, 30(12), 1213–1230.